Cellulose (2020) 27:2583–2597
https://doi.org/10.1007/s10570-019-02958-0

ORIGINAL RESEARCH

Boosting electrical properties of flexible PEDOT/cellulose fiber composites through the enhanced interface connection with novel combined small-sized anions

Ziyang Chang · Xianhui An · Xueren Qian

Received: 16 September 2019 / Accepted: 26 December 2019 / Published online: 10 January 2020

Abstract Rapid development of flexible electronics has raised the demand for renewable conductive materials. Biomass-derived cellulose fibers (CFs) are very promising candidates due to their outstanding advantages. In this paper, flexible, lightweight and freestanding biomaterial with high electrical conductivity was prepared via in situ chemical polymerization process using 3,4-ethylenedioxythiophene (EDOT) and CFs. In order to improve the performance of PEDOT/CFs, novel combined small-sized anion doping agents, sulphosalicylic acid (SSA) and sodium benzenesulfonate (SBS), were adopted to construct a well-organized conducting layer. The obtained PEDOT layer possessed good crystallinity and high doping level and was uniformly coated onto the surface of CFs through the dopant-dependent interface. The PEDOT:SSA-SBS/CFs exhibited electrical conductivity as high as 472 S/m and the mass loading was up to 1.92 mg/cm^2. Moreover, the flexible biomaterial displayed favorable electrochemical stability. Hence, the results presented here provide a new way to produce highly conducting and flexible biomaterial.

Electronic supplementary material The online version of this article (https://doi.org/10.1007/s10570-019-02958-0) contains supplementary material, which is available to authorized users.

Z. Chang · X. An · X. Qian (✉)
Key Laboratory of Bio-based Materials Science and Technology of Ministry of Education, Northeast Forestry University, Harbin 150040, People's Republic of China
e-mail: qianxueren@aliyun.com

Graphic abstract

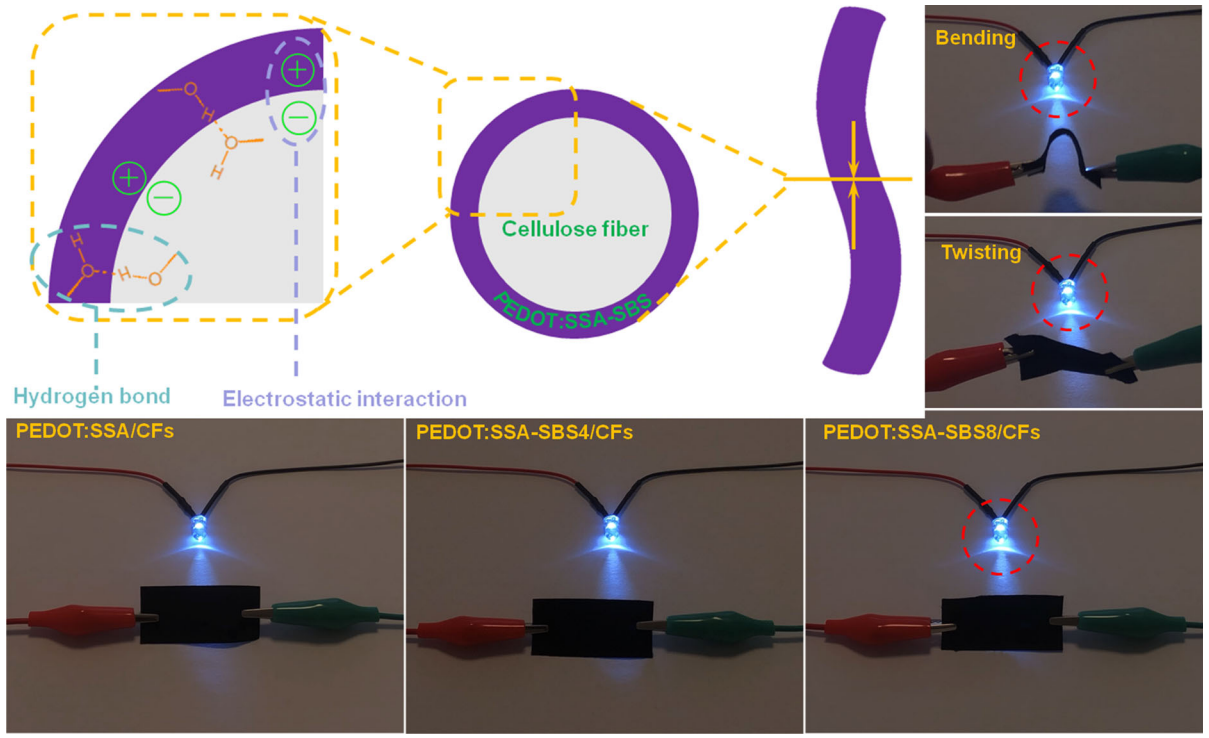

Keywords Electrical conductivity · Cellulose · Conductive polymer · Dopant · Organic electrical · Biomaterial

Introduction

Currently, in the rapid development of consumer electronics, an urgent demand for the development of flexible smart electronics and energy storage apparatus is expected (Nyholm et al. 2011). Petrochemical-based products, metal and inorganic semiconductors can meet the fundamental requirements (Du et al. 2017). However, the huge consumption of these traditional raw materials inevitably leads to visible and invisible environmental problems. One is the enormous amount of nondegradable discarded devices, for another is the excessive consumption of rare natural resources, for instance the use of indium, selenium and gallium led to the resource shortage (Du et al. 2017). Organic semiconductors meet the requirements of flexible smart electronics and energy storage apparatus due to their easy production, conductivity and excellent capacitance (Berggren et al. 2007). However, the natural brittleness and low conductivity limit their applications (Chang et al. 2019). In order to reduce or eliminate the negative impact on environment and build a sustainable world, inexpensive, renewable and biodegradable biomaterials, such as carbohydrate polymers, chitosan and vegetable protein, are being increasingly developed to replace the traditional materials to fabricate electronic apparatus (Irimia-Vladu 2014).

As the skeleton of plants, cellulose is one of the most plentiful carbohydrate polymers and promising natural biomaterials due to its cheapness, renewability and environmental friendliness (Agate et al. 2018). Cellulose fibers (CFs), separated from wood, cotton and agriculture byproducts by chemical and/or mechanical process, have been used as papers and textiles for thousands of years due to their renewable, light-weight and economical performance (Hinterstoisser et al. 2003). Moreover, the reliable stability and rich reactive hydroxyls of CF substrates allow the incorporation of advanced functional materials and nanotechnologies. Compared to cellulose fibers in nano size, CFs used as substrates are more energy

saving, ecofriendly and easier to industrialization because the preparation of nanocellulose consumes a lot of chemicals. Furthermore, it also enables fabrication of flexible devices, including in flexible smart electronics and energy storage apparatus, owing to the flexible nature of CFs which were separated from natural plants. Recently, the CF-based composites have been regarded as prospective platform for portable and inexpensive devices as the CFs are widely available, biodegradable and can be folded or rolled into desired configurations (Feng et al. 2014; Hamedi et al. 2016; Jur et al. 2011). However, the intrinsical insulation of CFs, which makes integration of functional electronic counterparts difficult is the major concern for functional devices fabrication. To overcome this limitation, many researchers have concentrated on developing conducting CF substrates by combining conductive materials with CFs. Recently, inorganic nanoparticles [layered boron nitride (Zhu et al. 2014), ZnO (Jur et al. 2011), tin-doped indium oxide (Hu et al. 2013)], metal nanoparticles/nanowires [copper nanowire (Jason et al. 2015), silver nanoparticle (Janrungroatsakul et al. 2013), silver nanowire (Hu et al. 2013), Au nanoparticle (Ko et al. 2017)], carbon materials [graphene (Hou et al. 2018), carbon nanotubes (Anderson et al. 2010)], conductive polymers (Anothumakkool et al. 2015; Chen et al. 2011; Fei et al. 2019; Huang et al. 2006; Li et al. 2010; Wan et al. 2017; Yuan et al. 2013; Zhang et al. 2017) and their multi-components (Tsai et al. 2019; Zhao et al. 2017) have been associated with CFs to form conducting materials. In this way, CF-based conducting materials incorporating the specific conducting properties and the characteristic properties of CFs could be fabricated.

Among a variety of conducting materials, PEDOT has been one of the most commonly used conducting additives for conducting CFs, because of its outstanding electrical conductivity and biocompatibility (Alhashmi Alamer 2018; Anothumakkool et al. 2015; Hamedi et al. 2016; Han et al. 2019; Wang et al. 2016). In addition, conducting CFs based on PEDOT can be readily fabricated via spin coating, brush coating or dipping coating using commercially available PEDOT:PSS aqueous solution (Koutsouras et al. 2017). However, there is only a weak van der Waals' force between PEDOT:PSS and CFs in the coating methods aforementioned. In the commercial PEDOT:PSS aqueous solution, the short chains of hydrophobic PEDOT aggregated into nanoparticles. And the nanoparticles were wrapped with long chains of hydrophilic PSS to get hydrophilicity. Thus, only a fraction of deprotonated styrene sulfonate groups are close enough to conjugated EDOT moieties as dopants (Berggren et al. 2007; Takano et al. 2012). On the one hand, the insulting PSS chains in PEDOT:PSS may occupy a substantial volume in the conductive channels and/or hinder charge transport in PEDOT chains, resulting in poor electrical performance (Kim et al. 2018). The same time, the steric effect of large polyanion segments in PSS may form amorphous structure and affect performance of conduting PEDOT/CFs (Li et al. 2019; Saxena et al. 2019; Shi et al. 2018). For versatile applications of flexible PEDOT/CF substrates, achieving a high electrical conductivity is necessary. Therefore, there is great potential for PEDOT doped with small-sized dopants because of the compact and order structure of PEDOT:small-sized anion (Chueh et al. 2017; Gueye et al. 2016; Shi et al. 2015, 2017; Tsakova et al. 2015). In addition, among the various methods available for conducting PEDOT/CFs preparation, the simple and common in situ polymerization technique was considered as the suitable candidate for scalable production of high conducting CFs.

Herein, we report a flexible, lightweight and freestanding biomaterial from CFs and PEDOT, which is prepared via one-step in situ chemical polymerization process. To optimize the interfacial performance of PEDOT with CFs for high electrical conductivity, novel combined small-sized anions, sulphosalicylic acid (SSA) and sodium benzenesulfonate (SBS), were introduced into PEDOT/CFs to replace the commonly used PSS. SSA not only acted as small-sized dopant, but also performed as binder to improve the interfacial conection between PEDOT and CFs. Meanwhile, the SBS is regarded as a surfactant to enhance the solubility of EDOT monomer in aqueous solution, and it also improved the doping level and crystallinity by doping in chains of PEDOT. The electrical conductivities of PEDOT:SSA-SBS/CFs were optimized by adjusting reaction conditions. Morphology, structures and properties of conducting PEDOT:SSA-SBS/CFs were systematically studied. This strategy may shed new light on the production of low cost and ecofriendly conducting materials for versatile applications.

Experimental section

Materials

Cellulose fibers (CFs, bleached softwood kraft pulp) were provided by Hengfeng Paper Co., Ltd. (Heilongjiang, China) and beaten to 42 °SR in a Valley beater before use. 3,4-Ethylenedioxythiophene (EDOT, ≥ 98%) was purchased from ShangHai D&B Biological Science and Technology Co., Ltd. (Shanghai, China). All other chemicals were purchased from Shanghai Aladdin Chemical Reagent Inc., and were used without further purification. All the solutions were prepared with distilled water.

Preparation of PEDOT:SSA-SBS/CFs conducting biomaterial

The PEDOT/CFs were prepared via one-step in situ chemical polymerization process according to the literature with some modifications (Wang et al. 2016). Typically, CFs (2 g, oven dry weight) were dispersed in EDOT aqueous solution (20 mmol, 150 ml) containing desired amount of SSA and SBS, and stirred for 20 min at room tempreture. Subsequently, 50 mL ammonium persulfate aqueous solution (APS, the molar ratio of APS to EDOT was 1:1) was dropwise added as an initiator for the polymerization process. The reactions were carried out in a water bath at 50 °C with stirring for 24 h. The resulted samples were collected by filter and washed with tap water in a nylon filter bag (100 meshs) until the filtrates became colorless to remove the unstable adsorbed polymers on CFs. The handsheets were prepared from PEDOT/CFs on a ZCX-200 handsheet former. The wet handsheets were then pressed at 0.4 MPa for 6 min (3 min each side) and dried at 105 °C for 10 min (each side 5 min) (Ding et al. 2010). Finally, flexible conducting biomaterials of PEDOT:SSA-SBS/CFs were obtained. The control sample PEDOT:SSA/CFs was prepared with the same process in the absence of SBS.

Measurement of electrical conductivity

The bulk resistivities (ρ, Ω cm) were measured with a RTS-8 four-point probes resistivity measurement apparatus. Since the ρ is related with the dimension of paper sample, the thickness (t, mm) and grammage (W, g/m^2) were measured beforehand. The conductivity (k, S/m) of paper sample was calculated according to the equation $k = 100/\rho$.

Calculation of the mass loading of PEDOT:SSA-SBS

The mass loading of PEDOT:SSA-SBS on CFs was determined according to the following equation:

$$\text{Mass loading}\left(\text{mg/cm}^2\right) = (W - W_0)/10$$

where W_0 is the grammage of blank paper with only cellulose fibers, g/m^2 and W is the grammage of paper with PEDOT/CFs, g/m^2.

Electrochemical characterization

Electrochemical stability of representative paper sample from PEDOT:SSA-SBS/CFs prepared at EDOT monomer concentration of 0.1 mol/L, SSA of 0.3 mol/L, n(SBS)/n(EDOT) = 0.4, n(APS)/n(EDOT) = 1 was evaluated on a CHI 660E electrochemical workstation (CH Instruments Inc., China). Cyclic voltammetry (CV) tests were conducted from − 0.1 to 0.9 V in 1 M H_2SO_4 aqueous solution. The electrochemical impedance spectroscopy (EIS) tests were performed from 0.01 Hz to 100 kHz with an amplitude of 5 mV. The freestanding conductive paper samples were cut into square strips with a typical area about 10 mm × 10 mm and then directly clamped in a polytetrafluoroethylene chuck with a platinum plate as working electrodes without any binder and conducting additive. A platinum plate and a Ag/AgCl electrode were performed as counter and reference electrodes, respectively.

Hydrophilicity evaluation

The measurement of contact angles (CA) with 5 μL water droplets were performed using a commercial contact meter (Powreach, JC2000C) at ambient temperature to evaluate the hydrophilicity of CFs, PEDOT:SSA/CFs and PEDOT:SSA-SBS/CFs.

Measurement of EMI shielding efficiency

The electromagnetic interference shielding effectiveness (EMI SE) of the paper samples were measured

with an Agilent E4402B spectrum analyzer and standard butt coaxial cable line with flange. The shielding effectiveness value was calculated as: $SE = -10 \times \lg(P_{out}/P_{in})$, where P_{out} and P_{in} are the incident and transmitted power, respectively.

SEM, ATR-FTIR, XPS, XRD and TGA characterization

A scanning electron microscope (SEM, JSM-7500F, Japan) was used to observe the morphology of conducting biomaterials. Attenuated total reflectance-fourier transform infrared (ATR-FTIR) spectra were collected over a range of 550–4000 cm^{-1} on a Thermo Fisher Scien-tific Nicolet 6700 spectrometer with a resolution of 4 cm^{-1} and scanning frequency of 32 times. The doping level of PEDOT was determined by X-ray photoelectron spectroscopy (XPS, Kratos AXIS SUPRA, England). The crystal structures of the materials were characterized using X-ray diffractometer (XRD, D/max 2200, Rigaku, Japan) with Ni-filtered Cu K radiation (1.5406 Å) at 40 kV and 40 mA. Scattered radiation was detected in the range of $2\theta = 5° - 40°$ at a scan rate of 4° min^{-1}. The thermal stabilities were measured using a thermogravimetric analyzer (TGA, Pyris 6, PerkinElmer, USA) from 50 to 800 °C at a heating rate of 10 °C min^{-1} in a nitrogen environment.

Results and discussion

Preparation of small-sized anions doped PEDOT on CFs

The chemical structures of SSA, SBS and EDOT are presented in Fig. 1a, which were employed in the preparation of highly conducting PEDOT layer on CFs. As shown in Fig. 1c, CFs serve as backbone in PEDOT:SSA-SBS/CFs. Rich surface hydroxyls enable CFs became competitive substrates for the incorporation of functional materials. It is noticeable, however, the hydrophobicity of PEDOT makes it diffcult to directly deposite on hydrophilic CFs. Thus, the monomer might tend to polymerize and agglomerate in solution instead of on the surface of CFs (Zhuang et al. 2018). Traditionally, PEDOT was doped with PSS to improve the hydrophilicity (Fig. 1b) in order to realize the excellent water processability. However, limited conductivity as well as amorphous structure of PEDOT was resulted from the excessive intrinsic insulating PSS in the polymer matrix. Compared to PEDOT:PSS, PEDOT doped with small-sized anions has greater potential for electrical applications.

Because of the interesting structure of SSA, it was selected to combine with SBS as co-dopants to improve the hydrophilicity of PEDOT as well as the interaction with CFs (Fig. 2). As an important element of the combined small-sized anion dopants, SSA not only served as dopant through the $–SO_3^-$ on one side of benzene ring, but also played a key role in the hydrogen bond formation with CFs through –OH and –COOH on the other side of benzene ring. Moreover, SSA provided an acidic environment which is essential for the oxidation of EDOT (Elschner et al. 2010).

In order to further improve the performance of PEDOT/CFs, as one of the smallest phenyl sulfonate, SBS was employed in the polymerization process. Regarding the chemical structure, SBS not only could be used as surfactant with amphipathicity to improve solubility of EDOT monomer in water, but also could be regard as an efficient dopant to enhance the doping level of PEDOT. In addition, according to previous reports, the structure, morphology and conductivity of PEDOT prepared by in situ chemical polymerization process are affected by surfactant (Han and Foulger 2006). In comparison with the system without surfactant, SBS could form micelles which including monomers into the core via phenyl hydrophobic ends while extending the hydrophilic sulfonic units into water to improve the dispersion of monomers in water (Zhuang et al. 2018). Typical samples obtained under different reaction conditions and results are shown in Table 1 and Table S1.

The EDOT monomers were transformed to oxidation state and sequentially formed cationic polymer after being oxidized by APS. The electronegative CFs were combined with cationic PEDOT through electrostatic interaction. Meanwhile, electronegative sulfonate groups from SSA and SBS were doped into the polymer chains during conductive layer formation (Fig. 2). Both the sulfonyl salicylate ions and benzene sulfonic ions acted as counterions for PEDOT coating on CFs. It is noteworthy that the affinity of PEDOT to CFs was improved after doped with SSA. The presence of SSA offered an extra interaction between hydrophilic CFs and hydrophobic PEDOT. In

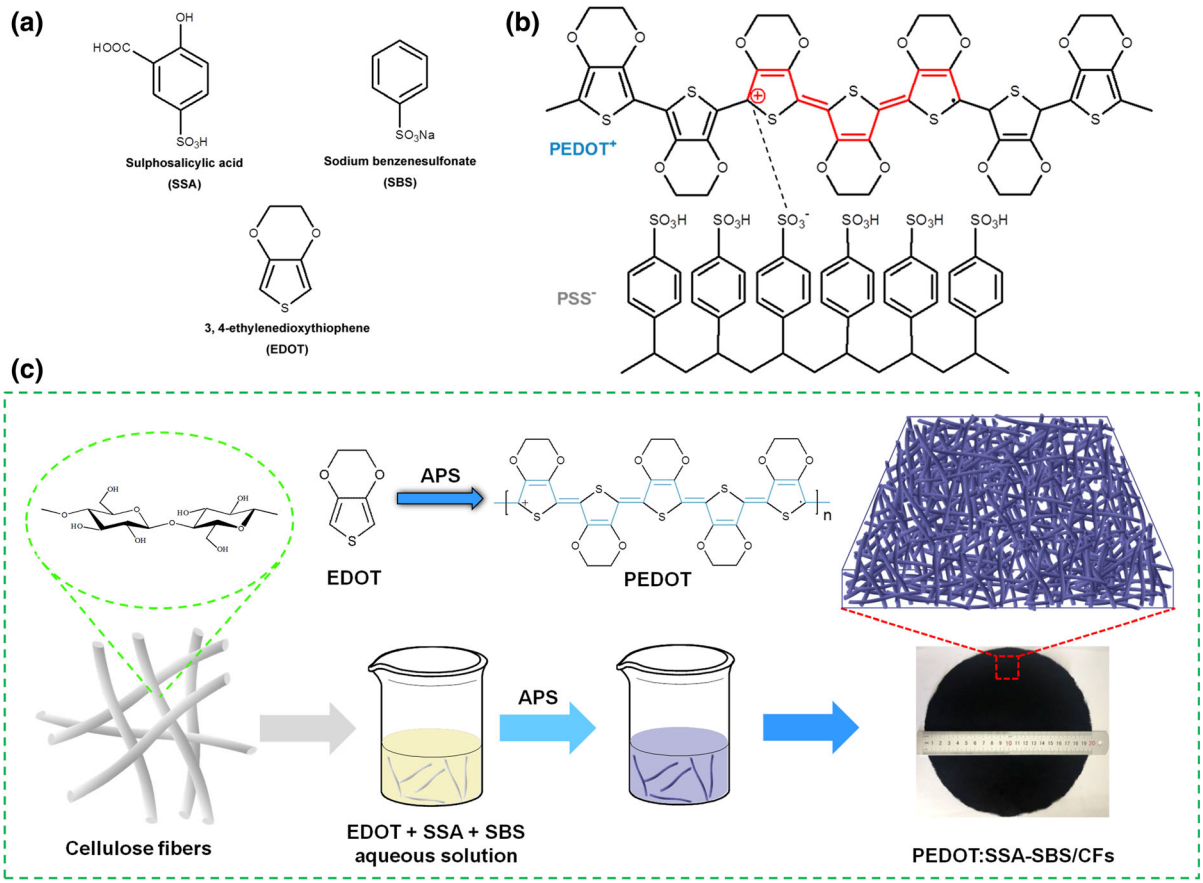

Fig. 1 **a** Chemical structure of SSA, SBS and EDOT. **b** Chemical structure of PEDOT:PSS complex. PEDOT: PSS complex consists of charge-neutralized core surrounded by excessive PSS that forms a hydrophilic shell (Petsagkourakis et al. 2019). **c** Schematic illustration of the preparation of flexible composite PEDOT:SSA-SBS/CFs

addition, it also led to a relatively well-coated PEDOT layer, which means the successful construction of conductive network on the CFs surface. And the formation of SBS micelles facilitated the uniform dispersed and high level doped PEDOT.

Morphology and structure

Morphological evaluation of pristine CFs and PEDOT deposited CFs were studied using SEM. It can be observed from the images that the surface of pristine CFs (Fig. 3a, e) displayed a smooth and clean morphology, whereas the roughness of PEDOT deposited surface was apprently higher. Figure 3b, f showed deposition of PEDOT:SSA on CFs, while PEDOT:SSA-SBS on CFs with 4 mmol and 8 mmol SBS were shown in Fig. 3c, g and d, h, respectively. The results confirmed that the CFs were successfully wrapped with a PEDOT layer. When PEDOT was doped with SSA only (Fig. 3b, f), the coating layer showed conventional apparent particles which tightly covered the surface of CFs. But, the polymer layer was scattered and the surface of CFs was not covered all (Figure S1a), which resulted a fair conductivity. After SBS addition, the solubility of EDOT was improved, which meaned the well dispersion of EDOT in aqueous solutin and then well polymerized on the surface of CFs. As shown in Figure S1b, c and d, the particle size was performed smaller and finer with the increase of SBS amount. At the amount of 8 mmol of SBS, the polymer layer displayed a smoother and well-organized morphology than the other two PEDOT/CFs samples. SSA and SBS both made contribution to the morphology of PEDOT coating, which led to a better conductivity.

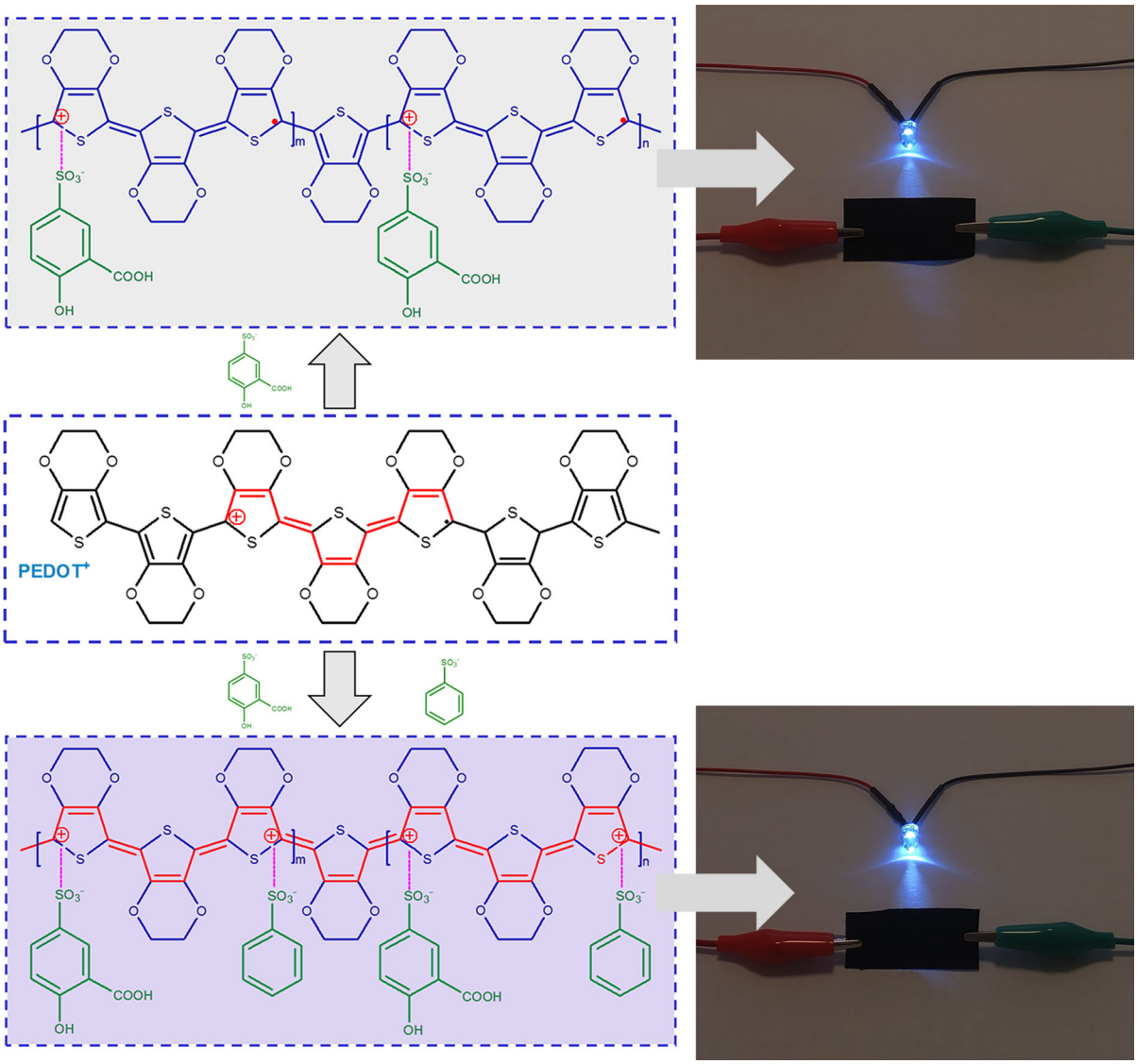

Fig. 2 Illustration of the small-sized doping agents in PEDOT

Table 1 Samples obtained under different reaction conditions

Sample	SSA mmol	SBS mmol	EDOT mmol	APS mmol	Electrical conductivity S/m	Mass loading of PEDOT mg/cm^2
PEDOT:SSA/CFs	60	0	20	20	33.13	1.11
PEDOT:SSA-SBS2/CFs	60	2	20	20	228.31	1.48
PEDOT:SSA-SBS4/CFs	60	4	20	20	366.30	1.71
PEDOT:SSA-SBS8/CFs	60	8	20	20	471.70	1.92

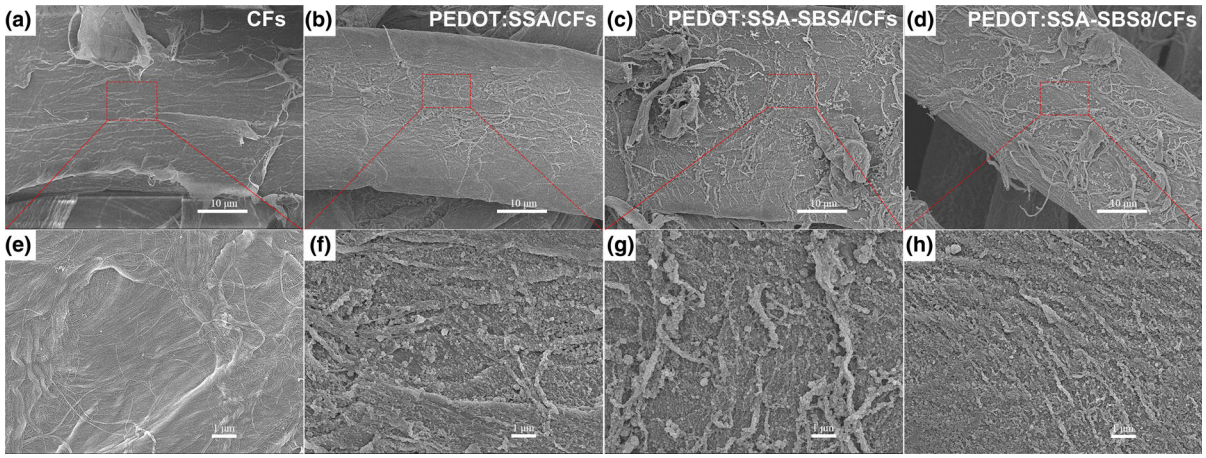

Fig. 3 SEM images of CFs (**a**, **e**), PEDOT:SSA/CFs (**b**, **f**), PEDOT:SSA-SBS4/CFs (**c**, **g**) and PEDOT:SSA-SBS8/CFs (**d**, **h**)

Figure 4a shows the influence of SSA concentration on the conductivity of the PEDOT:SSA/CFs and PEDOT:SSA-SBS8/CFs. The conductivity of PEDOT:SSA-SBS8/CFs increased as the amount of SSA increased and reached a maximum value of 472 S/m at the SSA amount was 60 mmol, which may attribute to the efficiency doping of the small-sized anions and interfacial connection between conductive polymer and CFs by SSA. The *k* of PEDOT:SSA/CFs and PEDOT:SSA-SBS8/CFs reached their maximum values at the same SSA concentration. This result suggests that the conductivity is affect by the concentration of SSA with a same doping mechanism. When the SSA amount ranges from 40 to 60 mmol, high conducivity are achieved, more than hundred times higher than that of PEDOT doped only with SSA. When the amount increased to 80 mmol, *k* was decreased sharply which may be caused by the polymerization of EDOT monomer in solution instead of on CFs. As the same concentration of SSA, SBS played key role to improve the conductivity of samples, which may attribute to the higher doping level and more regular structure (Kaphle et al. 2016; Shi et al. 2018).

To get clearer structures as well as the doping levels of PEDOT on CFs with different doping strategy, chemical analyses, including XRD, XPS and FTIR spectroscopy, were conducted. The XRD result (Fig. 4b) shows two strong peaks at 15.7° (110) and 22.5° (002) for the CFs, which are the characteristic peaks of cellulose (Anothumakkool et al. 2015). Compared to CFs, the relative intensity of the two characteristic peaks at 15.7° and 22.5° of PEDOT:SSA/CFs and PEDOT:SSA-SBS8/CFs are decreased gradually. This is attribute to higher mass loading and better uniformity of the PEDOT:SSA-SBS8 than PEDOT:SSA on CFs. Beyond the peaks mentioned above, characteristic peaks of PEDOT were observed in PEDOT:SSA/CFs and PEDOT:SSA-SBS8/CFs. The peaks at 6.5° and 26.2° are corresponding to the (100) and (020) planes, respectively, which are in accordance with the pervious reports (Anothumakkool et al. 2015; Kim et al. 2018; Migliaccio et al. 2019). The (100) spacing is in relation with the inter π-conjugated chain distance of the staked PEDOT polymer. Interestingly, the relative intensity of (100) and (020) planes of PEDOT:SSA-SBS8/CFs are all higher than that of PEDOT:SSA/CFs, which represented a higher crystallinity of PEDOT chains in PEDOT:SSA-SBS8/CFs. This serves as an indirect evidence for the existence of more ordered structure in PEDOT:SSA-SBS8/CFs, which promotes the better interchain interaction and, thereby, efficient charge transfer between the chains compared to PEDOT:SSA/CFs (Anothumakkool et al. 2015; Kim et al. 2006).

The conductivity of PEDOT was partially determined by the extent of electron removal from the charge-neutralized polymer chains. Such the positive charges created in the PEDOT chains are balanced by the counterions which are known as dopants (Anothumakkool et al. 2015; Elschner et al. 2010). So, the conductivity of polymer could be enhanced by increasing the delocalized electron in the chains. The

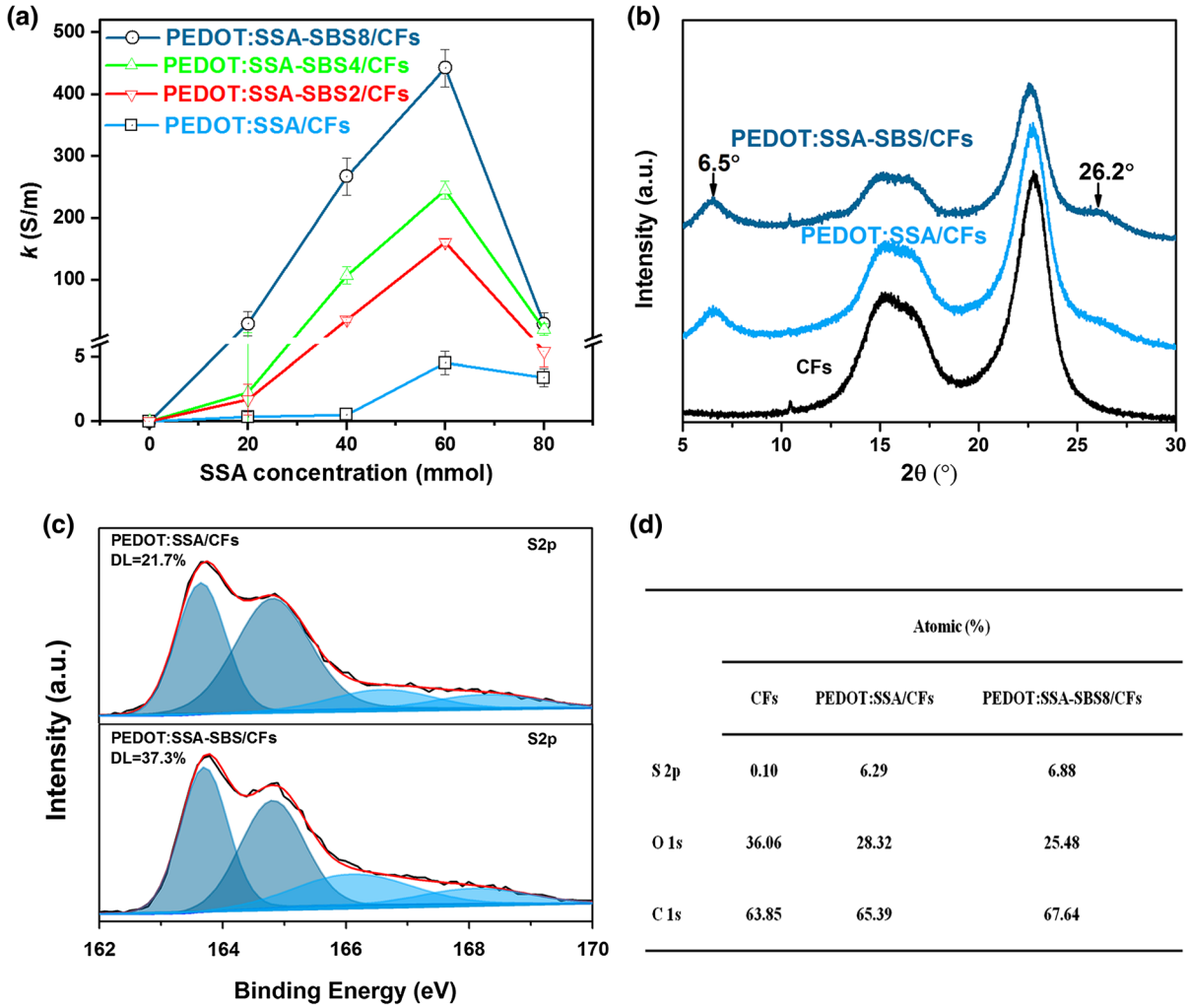

	Atomic (%)		
	CFs	PEDOT:SSA/CFs	PEDOT:SSA-SBS8/CFs
S 2p	0.10	6.29	6.88
O 1s	36.06	28.32	25.48
C 1s	63.85	65.39	67.64

Fig. 4 **a** Influence of SSA concentration on the conductivity of the PEDOT:SSA/CFs, PEDOT:SSA-SBS2/CFs, PEDOT:SSA-SBS4/CFs and PEDOT:SSA-SBS8/CFs. **b** XRD diffractograms of CFs, PEDOT:SSA/CFs and PEDOT:SSA-SBS8/CFs. **c** S 2p XPS of PEDOT:SSA/CFs and PEDOT:SSA-SBS8/CFs (*DL* doping level). **d** Elemental analysis by XPS of samples

evidence about the doping level has been obtained from the XPS spectra of PEDOT:SSA/CFs and PEDOT:SSA-SBS8/CFs presented (Shi et al. 2017, 2018). As shown in the Fig. 4c, the doublet peaks at high binding energy (170–164 eV) are from the sulfonate anion and the other two peaks at lower energy (166–163 eV) are from the thiophene chain (Hu et al. 2013; Shi et al. 2017, 2018). The doping levels are determined by the integral area ratio of two kinds of peaks. The PEDOT:SSA-SBS coating on CFs has a doping level of 37.3%, almost twice the doping level (21.7%) of the sample doped with SSA only. Thus, the higher conductivity of PEDOT:SSA-SBS/CFs could be reconfirmed by the increased doping level compared to PEDOT:SSA on CFs. The elements analysis by XPS of samples was shown in Fig. 4d. Compared to PEDOT:SSA/CFs, higher concentration of sulphur and carbon, and lower consentration of oxygen were observed in PEDOT:SSA-SBS/CFs, which also suggests SBS incorporation as well as a higher doping level. In conclusion, XPS serves as evidence of increased doping level, which facilitates the charge delocalization and results improved conductivity. Moreover, the more ordered PEDOT chains in PEDOT:SSA-SBS8/CFs have contributed for the efficient inter-chain charge transfer as substantiated by XRD. Thus, the above two factors ensure the

PEDOT:SSA-SBS/CFs to achieve an excellent conductivity.

Influence of the amount of SBS, APS and monomer

Figure 5a shows the FTIR spectra of CFs (curve A), PEDOT:SSA/CFs (curve B), PEDOT:SSA-SBS4/CFs (curve C) and PEDOT:SSA-SBS8/CFs (curve D). Compared to CFs, the characteristic peaks at 3335 cm^{-1}, 2890 cm^{-1}, 1641 cm^{-1} and 1026 cm^{-1} of cellulose are gradually weakening in curve B, C and D, which means the gradually well formd PEDOT layers on CFs. This result is corresponding to the mass loading of PEDOT shown in Table 1. In addition, B, C and D are all show the characteristic peaks at about 1536, 1505 and 1478 cm^{-1}, which are attribute to the stretching modes of C=C and C–C in the thiophene ring; the peaks at 1170, 1137 and 1081 cm^{-1} are due to C–O–C bond stretching in ethylenedioxy ring; and further vibrations from the C–S–C bond in the thiophene ring are also seen at about 958, 876 and 718 cm^{-1} (Ni et al. 2019).

Figure 5b indicates the influence of *n*(SBS)/*n*(EDOT) on *k*. The conductivity of biomaterials was benefited from the addition of SBS. The conductivity was enhanced as the SBS amount rose and reached the maximum value when the *n*(SBS)/*n*(EDOT) was 0.4,

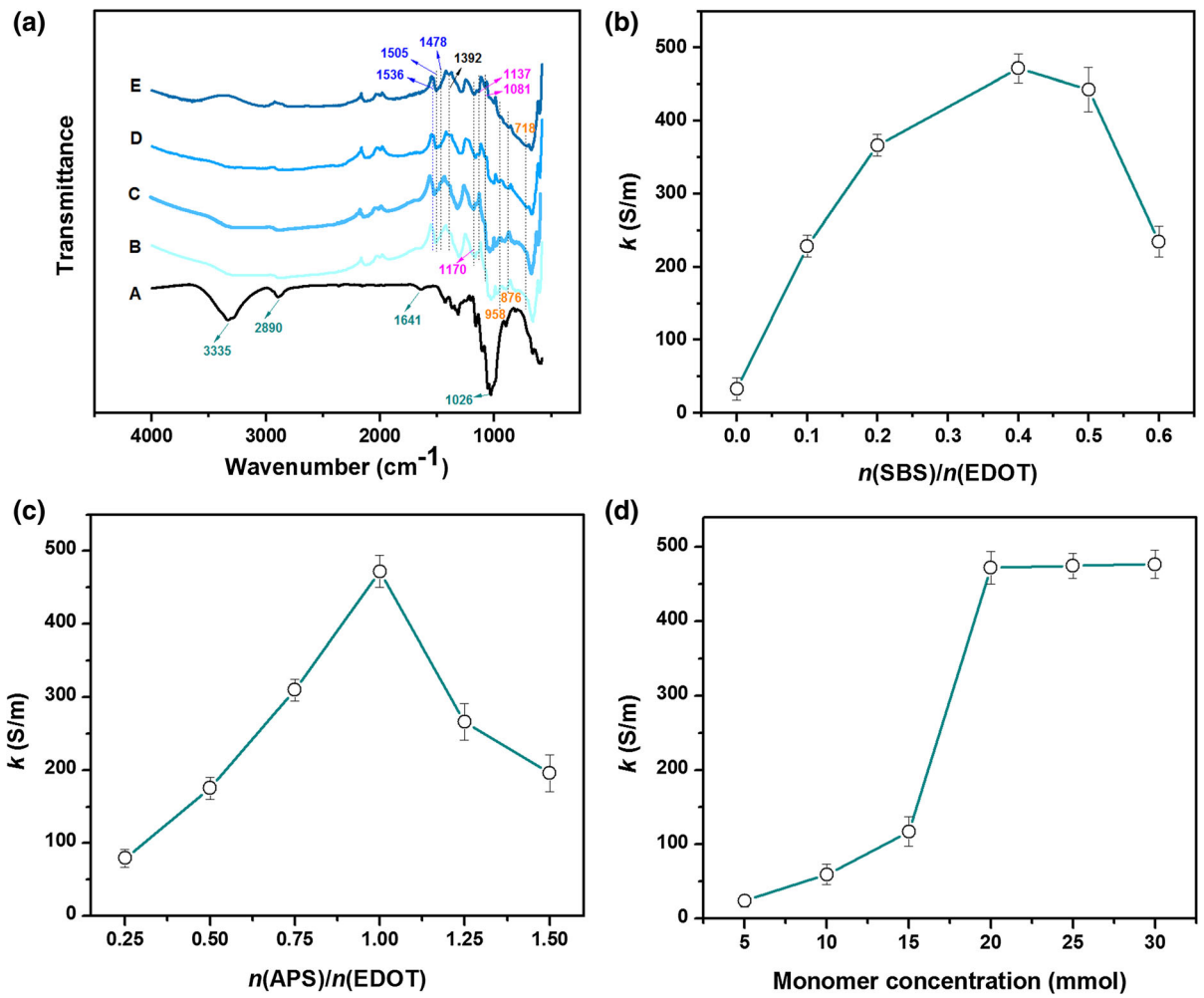

Fig. 5 **a** ATR-FTIR spectra of CFs (A), PEDOT:SSA/CFs (B), PEDOT:SSA-SBS2/CFs (C), PEDOT:SSA-SBS4/CFs (D) and PEDOT:SSA-SBS8/CFs (E). Influence of **b** *n*(SBS)/*n*(EDOT), **c** *n*(APS)/*n*(EDOT), and **d** monomer concentration on the *k* of PEDOT:SSA-SBS/CFs

which was attributed to the well-spread of EDOT as well as the PEDOT layer (Firuge 3 h). However, when the ratio increased to 0.5 and 0.6, the k decreased because of the agglomerated PEDOT (Figure S1). This result confirmed that the uniformity of PEDOT layer, crystallinity and doping level were vital for the conductivity of the PEDOT:SSA-SBS/CF composites which is corresponding to previous report (Zhuang et al. 2018). Figure 5c shows the k values of PEDOT:SSA-SBS/CFs with different n(APS)/n(EDOT). The conductivity was increased with APS increasing, which is simply explained by the increased oxidation degree of the samples when adding more APS. It could be observed that the maximum value *of k* reached when the ratio comes to 1.0. As a rule, lack of oxidant may result in incomplete polymerization of EDOT monomer. On the contrary, peroxidation could occur when excess oxidant was added, which could be verified in this study. It can be seen that the k decreased significantly from the maximum value when the n(APS)/n(EDOT) exceeded 1.0 owing to the peroxidation which was caused by the excess APS. As shown in Fig. 5d, it is obvious that the conductivity of the PEDOT:SSA-SBS/CFs was significantly affected by the monomer concentration. The conductivity went up apparently firstly and subsequently became almost constant at the end. Thus, 20 mmol EDOT can be regarded as the optimum monomer amount in the condition of our experiment in the presence of a certain amount of CFs.

Electrochemical, EMI, TGA characterization, hydrophilicity and flexibility evaluation

In this study, cyclic voltammograms (CV) and electrochemical impedance spectra (EIS) were conducted to assess the electrochemical stability of PEDOT:SSA/CFs and PEDOT:SSA-SBS8/CFs. The samples were firstly evaluated by CV with different cycle numbers (Fig. 6a). With the cycle number increased from 10 to 200, the area of PEDOT:SSA-SBS8/CFs showed a slight decrease. After 400 cycles, the curve maintained a similar shape. Furthermore, good symmetry can be observed from the curves, which indicated that the PEDOT:SSA-SBS8/CFs had good reversibility (Zhuang et al. 2018). In addition, compared to PEDOT:SSA/CFs, the curves of PEDOT:SSA-SBS8/CFs showed times higher area, which represented the excellent specific capacitance of PEDOT:SSA-SBS8/CFs. The Electrochemical impedance spectra (EIS) results were presented in Fig. 6b, which showed that the inherent resistance (R_s) value were 1.9, 2.8, 3.1 and 5.2 Ω of PEDOT:SSA-SBS8/CFs, PEDOT:SSA-SBS4/CFs, PEDOT:SSA-SBS2/CFs and PEDOT:SSA/CFs, respectively. The results indicated that the doping of combined anions significantly reduced the internal resistance and improved charge transfer of PEDOT layer on CFs. Overall, it could be found that the PEDOT:SSA-SBS8/CFs had attractive charge storage ability and electrochemical stability, indicating its potential for application in electronics and electrochemical biosensors. The electromagnetic interference (EMI) shielding effectiveness of the samples was presented in Fig. 6c. The EMI shielding effectiveness values are approximately 0 and 6 dB, corresponding to CFs and PEDOT:SSA/CFs, respectively, while the value of PEDOT:SSA-SBS8/CFs can reach as high as over 25 dB. It indicates that the EMI shielding efficiency could be effectively improved by doping PEDOT with the SSA and SBS. The result confirmed the abundant charge transfer and highly conducting ability of PEDOT:SSA-SBS8/CFs. The TGA was performed to evaluate the themal stability of samples. It can be seen that the residue char at 800 °C of PEDOT:SSA-SBS8/CFs was higher than the other two samples, as shown in Fig. 6d, which benefits the superior flame retardancy for the SSA and SBS doped PEDOT. Generally, the performance of electronics and biosensors were significantly affected by the wettability of fundamental materials (Hu and Cui 2012). Figure 6e showed that the hydrophilic groups of SSA and SBS contributed significantly to maintain the hydrophilicity of CFs. The excellent hydrophilicity character of conducting PEDOT:SSA-SBS8/CFs makes it a competitive material in the electronic application. In addition, as shown in Fig. 6f, the PEDOT:SSA-SBS8/CFs can be folded and twisted, and the LEDs were lighted well and there was no obvious difference in the light intensity, verifying the excellent flexibility and conductivity of the biomaterials. In addition, the papersheet showed no apparent crack after fold (Figure S2) indicating the excellent structural stability (Liu et al. 2018).

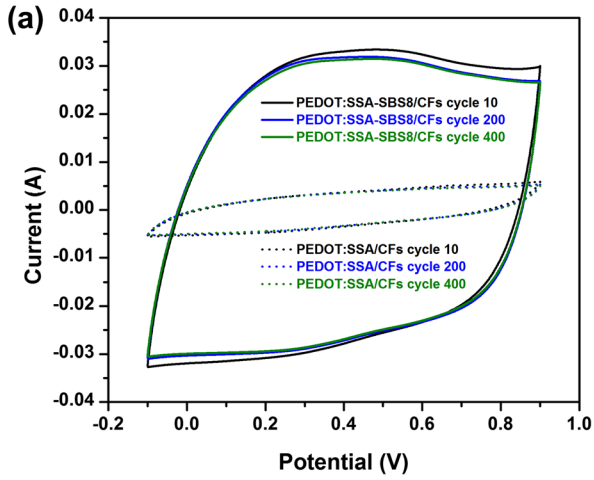
(a)
Current (A)
Potential (V)
PEDOT:SSA-SBS8/CFs cycle 10
PEDOT:SSA-SBS8/CFs cycle 200
PEDOT:SSA-SBS8/CFs cycle 400
PEDOT:SSA/CFs cycle 10
PEDOT:SSA/CFs cycle 200
PEDOT:SSA/CFs cycle 400

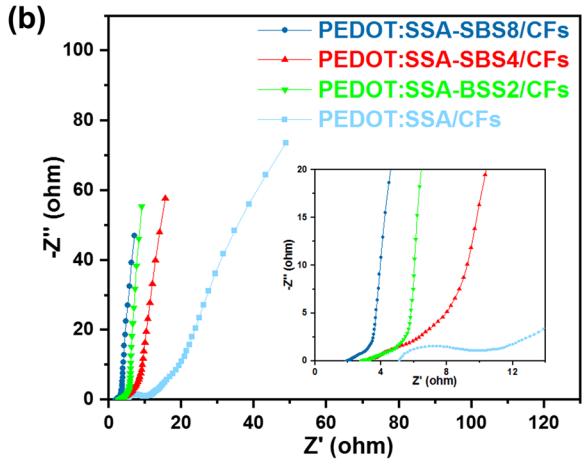
(b)
PEDOT:SSA-SBS8/CFs
PEDOT:SSA-SBS4/CFs
PEDOT:SSA-BSS2/CFs
PEDOT:SSA/CFs
-Z'' (ohm)
Z' (ohm)

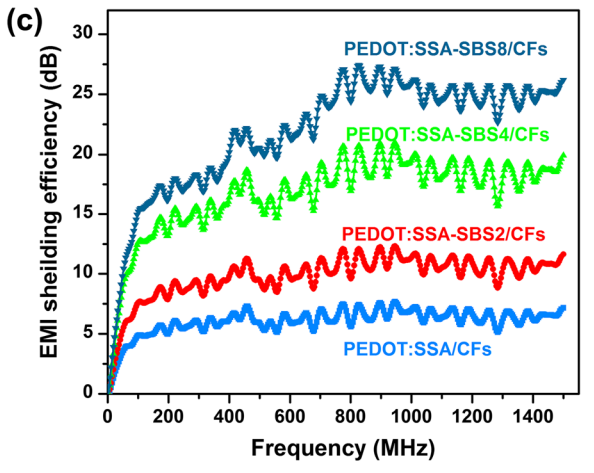
(c)
EMI sheilding efficiency (dB)
Frequency (MHz)
PEDOT:SSA-SBS8/CFs
PEDOT:SSA-SBS4/CFs
PEDOT:SSA-SBS2/CFs
PEDOT:SSA/CFs

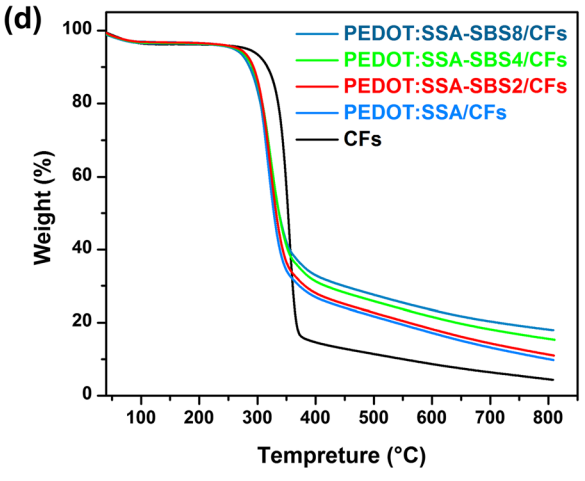
(d)
Weight (%)
Tempreture (°C)
PEDOT:SSA-SBS8/CFs
PEDOT:SSA-SBS4/CFs
PEDOT:SSA-SBS2/CFs
PEDOT:SSA/CFs
CFs

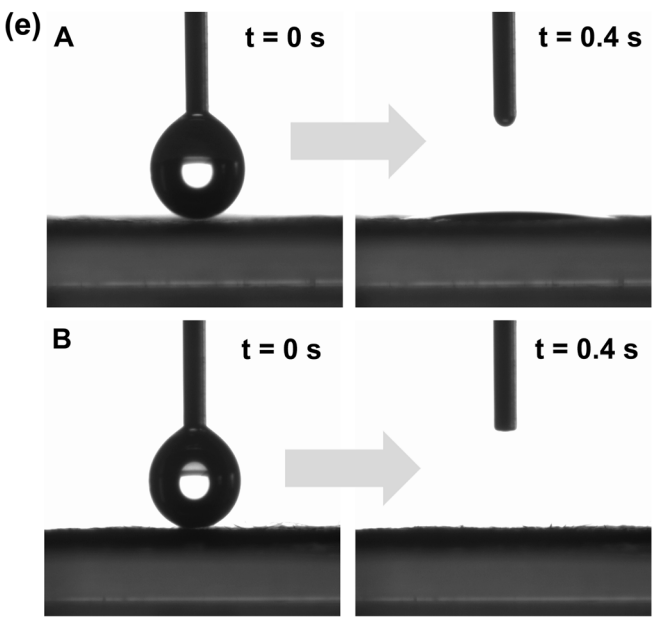
(e)
A
t = 0 s
t = 0.4 s
B
t = 0 s
t = 0.4 s

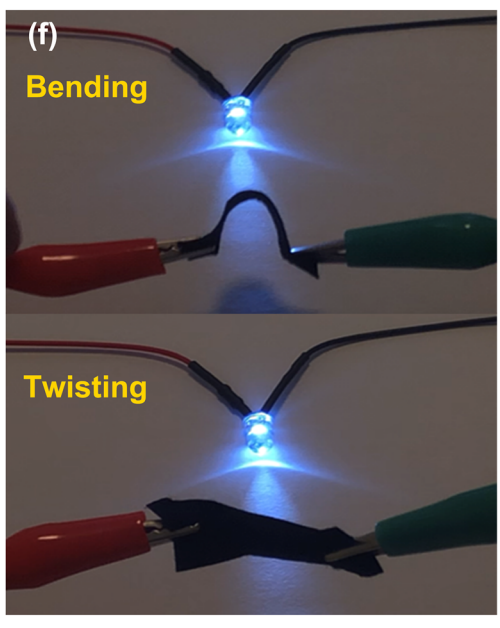
(f)
Bending
Twisting

◀**Fig. 6** **a** Cyclic voltammograms stability of PEDOT:SSA/CFs and PEDOT:SSA-SBS8/CFs with 10, 100 and 400 cycles at scan rate of 0.1 V/s, respectively. **b** Electrochemical impedance spectra of PEDOT:SSA/CFs, PEDOT:SSA-SBS2/CFs, PEDOT:SSA-SBS4/CFs and PEDOT:SSA-SBS8/CFs. **c** EMI shielding effectiveness study of PEDOT:SSA/CFs, PEDOT:SSA-SBS2/CFs, PEDOT:SSA-SBS4/CFs and PEDOT:SSA-SBS8/CFs (0–1.5 GHz). **d** TGA curves of CFs, PEDOT:SSA/CFs, PEDOT:SSA-SBS2/CFs, PEDOT:SSA-SBS4/CFs and PEDOT:SSA-SBS8/CFs. **e** Hydrophilicity of CFs and PEDOT:SSA-SBS8/CFs. **f** Lighting of a LED using the PEDOT:SSA-SBS8/CFs under bending and twisting

Conclusions

PEDOT doped with novel combined small-sized anions, SSA and SBS, was successfully prepared in the presence of CFs via a facile one step in situ chemical oxidative polymerization in aqueous solution, and resulted a flexible and highly conducting PEDOT:SSA-SBS/CFs biomaterial. The novel combined small-sized dopants, SSA and SBS were successfully used to improve the properties of PEDOT:SSA-SBS/CFs. In particular, the PEDOT layer was uniformly coated onto the surface of CFs through dopant-dependent interface by SSA addition. And SBS was regarded as surfactant to improve the dispersibility of EDOT monomer and doping level of PEDOT. The optimized electrical conductivity can reach up to 472 S/m with n(SSA)/n(EDOT) = 3 and n(SBS)/n(EDOT) = 0.4 owing to the good crystallinity and high doping level of PEDOT, which is much higher than that of other reported conductive polymer/natural substrate composites. The PEDOT:SSA-SBS/CFs also possess excellent electrochemical stability, EMI shielding effectiveness, themal stability, wetability and flexibility. As a result, the presented facile strategy may shed new light on the developing of biobased flexible electronics and biosensor probes.

Acknowledgments The authors gratefully acknowledge the National Natural Science Foundation of China (Grant No. 31770620) for financial support to this work.

Compliance with ethical standards

Conflict of interest The authors declare no competing financial interest.

References

Agate S, Joyce M, Lucia L, Pal L (2018) Cellulose and nanocellulose-based flexible-hybrid printed electronics and conductive composites—a review. Carbohydr Polym 198:249–260. https://doi.org/10.1016/j.carbpol.2018.06.045

Alhashmi Alamer F (2018) The effects of temperature and frequency on the conductivity and dielectric properties of cotton fabric impregnated with doped PEDOT:PSS. Cellulose 25(10):6221–6230. https://doi.org/10.1007/s10570-018-1978-x

Anderson RE, Guan J, Ricard M, Dubey G, Su J, Lopinski G, Dorris G, Bourne O, Simard B (2010) Multifunctional single-walled carbon nanotube–cellulose composite paper. J Mater Chem 20(12):2400–2407. https://doi.org/10.1039/b924260k

Anothumakkool B, Soni R, Bhange SN, Kurungot S (2015) Novel scalable synthesis of highly conducting and robust PEDOT paper for a high performance flexible solid supercapacitor. Energy Environ Sci 8(4):1339–1347. https://doi.org/10.1039/C5EE00142K

Berggren M, Nilsson D, Robinson ND (2007) Organic materials for printed electronics. Nat Mater 6(1):3–5. https://doi.org/10.1038/nmat1817

Chang Z, Li S, Sun L, Ding C, An X, Qian X (2019) Paper-based electrode comprising zirconium phenylphosphonate modified cellulose fibers and porous polyaniline. Cellulose 26(11):6739–6754

Chen Y, Qian X, An X (2011) Preparation and characterization of conductive paper via in situ polymerization of 3, 4-ethylenedioxythiophene. BioResources 6(3):3410–3423

Chueh CC, Li CZ, Ding F, Li Z, Cernetic N, Li X, Jen AK (2017) Doping versatile n-type organic semiconductors via room temperature solution-processable anionic dopants. ACS Appl Mater Interfaces 9(1):1136–1144. https://doi.org/10.1021/acsami.6b14375

Ding C, Qian X, Yu G, An X (2010) Dopant effect and characterization of polypyrrole-cellulose composites prepared by in situ polymerization process. Cellulose 17:1067–1077. https://doi.org/10.1007/s10570-010-9442-6

Du X, Zhang Z, Liu W, Deng Y (2017) Nanocellulose-based conductive materials and their emerging applications in energy devices—a review. Nano Energy 35:299–320. https://doi.org/10.1016/j.nanoen.2017.04.001

Elschner A, Kirchmeyer S, Lovenich W, Merker U, Reuter K (2010) PEDOT: principles and applications of an intrinsically conductive polymer. CRC Press, Boca Raton

Fei G, Wang Y, Wang H, Ma Y, Guo Q, Huang W, Yang D, Shao Y, Ni Y (2019) Fabrication of bacterial cellulose/polyaniline nanocomposite paper with excellent conductivity, strength, and flexibility. ACS Sustain Chem Eng 7(9):8215–8225. https://doi.org/10.1021/acssuschemeng.8b06306

Feng JX, Ye SH, Wang AL, Lu XF, Tong YX, Li GR (2014) Flexible cellulose paper-based asymmetrical thin film supercapacitors with high-performance for electrochemical energy storage. Adv Funct Mater 24(45):7093–7101. https://doi.org/10.1002/adfm.201401876

Gueye M, Carella A, Massonnet N, Yvenou E, Brenet S, Faure-Vincent J, Pouget S, Rieutord F, Okuno H, Benayad A, Demadrille R, Simonato J (2016) Structure and dopant engineering in PEDOT thin films: practical tools for a dramatic conductivity enhancement. Chem Mater 28(10): 3462–3468. https://doi.org/10.1021/acs.chemmater.6b01035

Hamedi MM, Campbell VE, Rothemund P, Güder F, Christodouleas DC, Bloch J-F, Whitesides GM (2016) Electrically activated paper actuators. Adv Funct Mater 26(15): 2446–2453. https://doi.org/10.1002/adfm.201505123

Han MG, Foulger SH (2006) Facile synthesis of poly(3,4-ethylenedioxythiophene) nanofibers from an aqueous surfactant solution. Small 2(10):1164–1169. https://doi.org/10.1002/smll.200600135

Han S, Alvi NUH, Granlof L, Granberg H, Berggren M, Fabiano S, Crispin X (2019) A multiparameter pressure-temperature-humidity sensor based on mixed ionic-electronic cellulose aerogels. Adv Sci 6(8):1802128. https://doi.org/10.1002/advs.201802128

Hinterstoisser B, Åkerholm M, Salmén L (2003) Load distribution in native cellulose. Biomacromolecules 4(5):1232–1237. https://doi.org/10.1021/bm030017k

Hou M, Xu M, Li B (2018) Enhanced electrical conductivity of cellulose nanofiber/graphene composite paper with a sandwich structure. ACS Sustain Chem Eng 6(3):2983–2990. https://doi.org/10.1021/acssuschemeng.7b02683

Hu L, Cui Y (2012) Energy and environmental nanotechnology in conductive paper and textiles. Energy Environ Sci 5(4):6423–6435. https://doi.org/10.1039/c2ee02414d

Hu L, Zheng G, Yao J, Liu N, Weil B, Eskilsson M, McGehee MD (2013) Transparent and conductive paper from nanocellulose fibers. Energy Environ Sci 6(2):513–518. https://doi.org/10.1039/c2ee23635d

Huang B, Kang G, Ni Y (2006) Preparation of conductive paper by in situ polymerization of pyrrole in a pulp fiber system. Pulp Pap Can 107(2):38–42

Irimia-Vladu M (2014) "Green" electronics: biodegradable and biocompatible materials and devices for sustainable future. Chem Soc Rev 43(2):588–610. https://doi.org/10.1039/C3CS60235D

Janrungroatsakul W, Lertvachirapaiboon C, Ngeontae W, Aeungmaitrepirom W, Chailapakul O, Ekgasit S, Tuntulani T (2013) Development of coated-wire silver ion selective electrodes on paper using conductive films of silver nanoparticles. Analyst 138(22):6786–6792. https://doi.org/10.1039/c3an01385e

Jason NN, Shen W, Cheng W (2015) Copper nanowires as conductive ink for low-cost draw-on electronics. ACS Appl Mater Interfaces 7(30):16760–16766. https://doi.org/10.1021/acsami.5b04522

Jur JS, Sweet WJ, Oldham CJ, Parsons GN (2011) Atomic layer deposition of conductive coatings on cotton, paper, and synthetic fibers: conductivity analysis and functional chemical sensing using "all-fiber" capacitors. Adv Funct Mater 21(11):1993–2002. https://doi.org/10.1002/adfm.201001756

Kaphle V, Liu S, Al-Shadeedi A, Keum CM, Lussem B (2016) Contact resistance effects in highly doped organic electrochemical transistors. Adv Mater 28(39):8766–8770. https://doi.org/10.1002/adma.201602125

Kim TY, Kim JE, Suh KS (2006) Effects of alcoholic solvents on the conductivity of tosylate-doped poly(3,4-ethylenedioxythiophene) (PEDOT-OTs). Polym Int 55(1):80–86. https://doi.org/10.1002/pi.1921

Kim SM et al (2018) Influence of PEDOT:PSS crystallinity and composition on electrochemical transistor performance and long-term stability. Nat Commun 9(1):3858. https://doi.org/10.1038/s41467-018-06084-6

Ko Y, Kwon M, Bae WK, Lee B, Lee SW, Cho J (2017) Flexible supercapacitor electrodes based on real metal-like cellulose papers. Nat Commun 8(1):536. https://doi.org/10.1038/s41467-017-00550-3

Koutsouras DA, Gkoupidenis P, Stolz C, Subramanian V, Malliaras GG, Martin DC (2017) Impedance spectroscopy of spin-cast and electrochemically deposited PEDOT:PSS films on microfabricated electrodes with various areas. ChemElectroChem 4(9):2321–2327. https://doi.org/10.1002/celc.201700297

Li J, Qian X, Chen J, Ding C, An X (2010) Conductivity decay of cellulose–polypyrrole conductive paper composite prepared by in situ polymerization method. Carbohydr Polym 82(2):504–509. https://doi.org/10.1016/j.carbpol.2010.05.036

Li X, Liu C, Zhou W, Duan X, Du Y, Xu J, Jiang Q (2019) Roles of polyethylenimine ethoxylated in efficiently tuning the thermoelectric performance of poly(3,4-ethylenedioxythiophene)-rich nanocrystal films. ACS Appl Mater Interfaces 11(8):8138–8147. https://doi.org/10.1021/acsami.9b00298

Liu Q, Chen Z, Jing S, Zhuo H, Hu Y, Liu J, Zhong L, Peng X, Liu C (2018) A foldable composite electrode with excellent electrochemical performance using microfibrillated cellulose fibers as a framework. J Mater Chem A 6:20338–20346. https://doi.org/10.1039/c8ta06635c

Migliaccio L, Altamura D, Scattarella F, Giannini C, Manini P, Gesuele F, Pezzella A (2019) Impact of eumelanin-PEDOT blending: increased PEDOT crystalline order and packing-conductivity relationship in ternary PEDOT:PSS: Eumelanin thin films. Adv Electron Mater 5(3):1800585. https://doi.org/10.1002/aelm.201800585

Ni D, Chen Y, Song H, Liu C, Yang X, Cai K (2019) Free-standing and highly conductive PEDOT nanowire films for high-performance all-solid-state supercapacitors. J Mater Chem A 7(3):1323–1333. https://doi.org/10.1039/c8ta08814d

Nyholm L, Nyström G, Mihranyan A, Strømme M (2011) Toward flexible polymer and paper-based energy storage devices. Adv Mater 23(33):3751–3769. https://doi.org/10.1002/adma.201004134

Petsagkourakis I, Kim N, Tybrandt K, Zozoulenko I, Crispin X (2019) Poly(3,4-ethylenedioxythiophene): chemical synthesis, transport properties, and thermoelectric devices. Adv Electron Mater. https://doi.org/10.1002/aelm.201800918

Saxena N, Pretzl B, Lamprecht X, Bießmann L, Yang D, Li N, Müller-Buschbaum P (2019) Ionic liquids as post-treatment agents for simultaneous improvement of seebeck coefficient and electrical conductivity in PEDOT:PSS

films. ACS Appl Mater Interfaces 11(8):8060–8071. https://doi.org/10.1021/acsami.8b21709

Shi W, Zhao T, Xi J, Wang D, Shuai Z (2015) Unravelling doping effects on PEDOT at the molecular level: from geometry to thermoelectric transport properties. J Am Chem Soc 137(40):12929–12938. https://doi.org/10.1021/jacs.5b06584

Shi W, Yao Q, Qu S, Chen H, Zhang T, Chen L (2017) Micron-thick highly conductive PEDOT films synthesized via self-inhibited polymerization: roles of anions. NPG Asia Mater 9(7):e405. https://doi.org/10.1038/am.2017.107

Shi W, Qu S, Chen H, Chen Y, Yao Q, Chen L (2018) One-step synthesis and enhanced thermoelectric properties of polymer–quantum dot composite films. Angew Chem 130(27):8169–8174. https://doi.org/10.1002/ange.201802681

Takano T, Masunaga H, Fujiwara A, Okuzaki H, Sasaki T (2012) PEDOT Nanocrystal in highly conductive PEDOT:PSS polymer films. Macromolecules 45(9):3859–3865. https://doi.org/10.1021/ma300120g

Tsai YJ, Wang CM, Chang TS, Sutradhar S, Chang CW, Chen CY, Liao WS (2019) Multilayered Ag NP-PEDOT-paper composite device for human-machine interfacing. ACS Appl Mater Interfaces 11(10):10380–10388. https://doi.org/10.1021/acsami.8b21390

Tsakova V, Ilieva G, Filjova D (2015) Role of the anionic dopant of poly(3,4-ethylenedioxythiophene) for the electroanalytical performance: electrooxidation of acetaminophen. Electrochim Acta 179:343–349. https://doi.org/10.1016/j.electacta.2015.02.062

Wan C, Jiao Y, Li J (2017) Flexible, highly conductive, and free-standing reduced graphene oxide/polypyrrole/cellulose hybrid papers for supercapacitor electrodes. J Mater Chem A 5(8):3819–3831. https://doi.org/10.1039/C6TA04844G

Wang Z, Tammela P, Huo J, Zhang P, Strømme M, Nyholm L (2016) Solution-processed poly(3, 4-ethylenedioxythiophene) nanocomposite paper electrodes for high-capacitance flexible supercapacitors. J Mater Chem A 4(5):1714–1722. https://doi.org/10.1039/C5TA10122K

Yuan L, Yao B, Hu B, Huo K, Chen W, Zhou J (2013) Polypyrrole-coated paper for flexible solid-state energy storage. Energy Environ Sci 6(2):470–476. https://doi.org/10.1039/c2ee23977a

Zhang Y, Li L, Zhang L, Ge S, Yan M, Yu J (2017) In-situ synthesized polypyrrole-cellulose conductive networks for potential-tunable foldable power paper. Nano Energy 31:174–182. https://doi.org/10.1016/j.nanoen.2016.11.029

Zhao D, Zhang Q, Chen W, Yi X, Liu S, Wang Q, Yu H (2017) Highly flexible and conductive cellulose-mediated PEDOT:PSS/MWCNT composite films for supercapacitor electrodes. ACS Appl Mater Interfaces 9(15):13213–13222. https://doi.org/10.1021/acsami.7b01852

Zhu H, Li Y, Fang Z, Xu J, Cao F, Wan J, Hu L (2014) Highly thermally conductive papers with percolative layered boron nitride nanosheets. ACS Nano 8(4):3606–3613. https://doi.org/10.1021/nn500134m

Zhuang A, Bian Y, Zhou J, Fan S, Shao H, Hu X, Zhang Y (2018) All-organic conductive biomaterial as an electroactive cell interface. ACS Appl Mater Interfaces 10(41):35547–35556. https://doi.org/10.1021/acsami.8b13820